Current Optics and Photonics
Vol. 4, No. 6, December 2020, pp. 540-544

ISSN: 2508-7266(Print) / ISSN: 2508-7274(Online)
DOI: https://doi.org/10.3807/COPP.2020.4.6.540

An Analysis on the Range of Singular Fusion of Augmented Reality Devices

Hanul Lee, Minyoung Park, Hyeontaek Lee, and Hee-Jin Choi*

Department of Physics and Astronomy, Sejong University, Seoul 05006, Korea

(Received September 29, 2020 : revised October 12, 2020 : accepted October 14, 2020)

Current two-dimensional (2D) augmented reality (AR) devices present virtual image and information to a fixed focal plane, regardless of the various locations of ambient objects of interest around the observer. This limitation can lead to a visual discomfort caused by misalignments between the view of the ambient object of interest and the visual representation on the AR device due to a failing of the singular fusion. Since the misalignment becomes more severe as the depth difference gets greater, it can hamper visual understanding of the scene, interfering with task performance of the viewer. Thus, we analyzed the range of singular fusion (RSF) of AR images within which viewers can perceive the shape of an object presented on two different depth planes without difficulty due to the failure of singular fusion. It is expected that our analysis can inspire the development of advanced AR systems with low visual discomfort.

Keywords : Augmented reality, Range of singular fusion, Visual discomfort
OCIS codes : (100.6890) Three-dimensional image processing; (110.2990) Image formation theory; (110.3000) Image quality assessment

I. INTRODUCTION

The augmented reality (AR) device is designed to project virtual information on the ambient object of interest. Thus, it is essential to align the AR information and the ambient object of interest so as to satisfy alignment accurately in order to increase the efficiency and safety by minimizing the movement of the primary gaze of the observer. In other words, a singular fusion of the AR information and the ambient object is necessary, which means a condition that the perception of two depth positions can be fused into a single view without diplopia (double vision) is a key factor to satisfy the above requirement. However, since current two-dimensional (2D) AR devices only present the virtual information to a fixed focal plane, the observer will recognize a misalignment between the 2D AR image and the object of interest due to the failure of singular fusion when there is a certain gap between them as shown in Fig. 1. Although Panum's fusional area is well known as a condition for comfort fusion without diplopia, the study cannot be directly applied for a viewing condition of current AR applications such as head-up display (HUD) or head-mounted display (HMD) because they project AR images at farther distances than for the cases of previous study [1].

In order to resolve the misalignment issue between the AR image and the real object described above, various approaches have been proposed. For example, an infinite focus technique turns out to be useful to prevent the problem of blurred vision [2]. The light field AR display technology is also expected to be a practical resolution to be commercialized in the near future [3-6]. In addition, the holographic AR display is also considered to be an ideal solution [7-10]. Nevertheless, even the latest 3D AR techniques described above still have limited accuracy when matching the positions of AR images with the real objects due to the limitations such as restricted design parameters of optical combiner and resolution of display devices. Besides, although it is understood that the accommodation-vergence (A-V) mismatch problem can be resolved by applying one of the 3D AR display techniques above [11], the misalignment shown in Fig. 1 due to the failed singular fusion can still induce a visual fatigue when the AR image and the real object are not within a range of singular fusion (RSF).

*Corresponding author: hjchoi@sejong.ac.kr, ORCID 0000-0002-6482-9358
Color versions of one or more of the figures in this paper are available online.

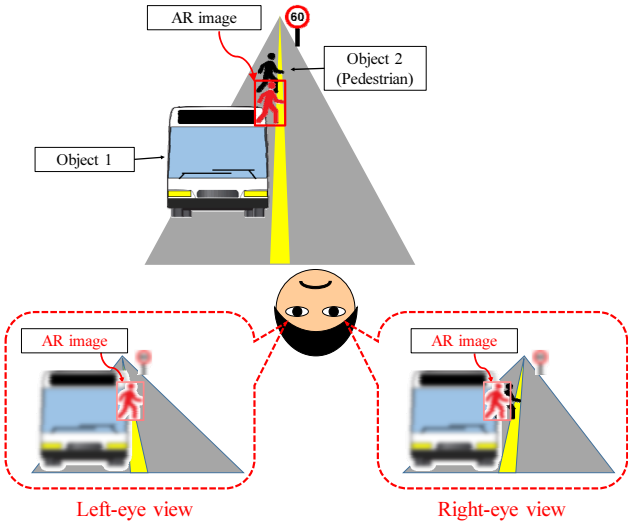

FIG. 1. A case with a failure of singular fusion of the ambient object (pedestrian) and the AR image.

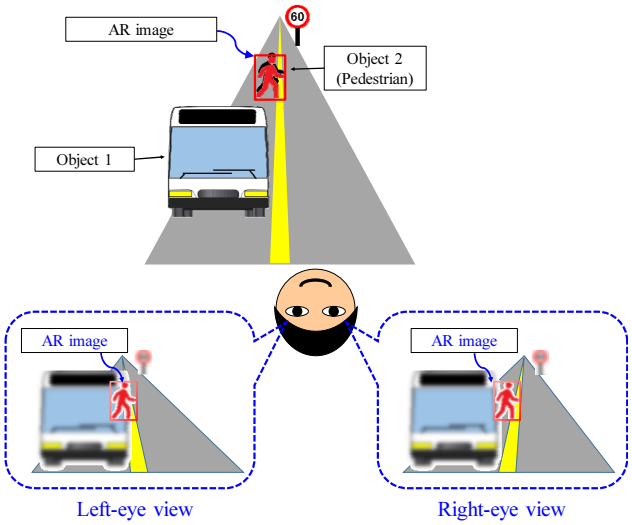

FIG. 2. A case with a singular fusion of the ambient object (pedestrian) and the AR image within the RSF.

Therefore, to develop advanced AR systems with low visual discomfort as shown in Fig. 2, it is necessary to analyze the RSF without recognizing the misalignment. For that purpose, we design an experimental scheme to derive the RSF with a practical viewing distance which can cover the projection range of current AR applications.

II. DESIGN OF EXPERIMENTAL SCHEME

As denoted above, we define the RSF as a range where both the AR image and the object within it can be combined together through a singular fusion without a diplopia. Thus, the experimental apparatus should provide a sensitive cue whether the observer succeeded or failed to achieve fusion. For that purpose, we designed a task-based experimental scheme to use two randomly encoded dot patterns as an AR image and a real image to include visual information of a single digit number from 0 to 9. Figure 3 shows some examples of the dot patterns encoded from an image of a single digit number.

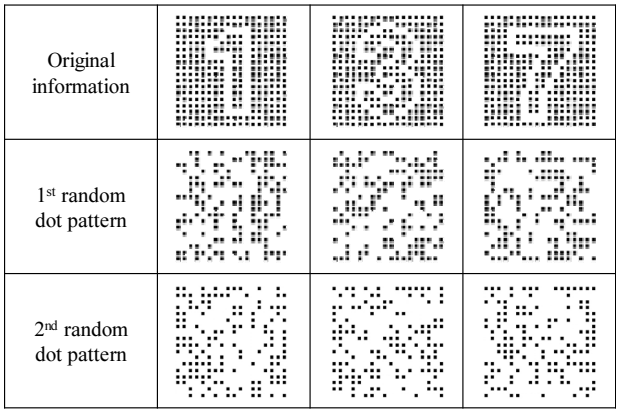

FIG. 3. Examples of randomly encoded patterns including an original information of a single digit number.

Figures 4(a) and 4(b) show the proposed experimental scheme. The 1st dot pattern is reflected by the beam splitter and shown to the observer as a virtual (AR) image, while the 2nd dot pattern is seen through the beam splitter as a real image. Thus, the observer can see an overlapped feature of those images as in using an HUD. Then, we asked the observer to fuse the dot patterns and answer what the single digit number (the original information) is. Since it is necessary for the observer to fuse the patterns at different locations accurately to decode the original information, we can determine whether the observer succeeded in making a singular fusion or not. In addition, to eliminate the effect of the previous trials, the random dot patterns are newly generated for every trial. Thus, we can assume that those dot patterns were inside the RSF when the observer responds with a correct answer as shown in Fig. 4(a). In contrast, if the observer was not able to respond with a correct single digit number, we assume that there is a failure of singular fusion and conclude that the real image is not within the RSF as shown in Fig. 4(b). As a result, by analyzing the proportion correct of the proposed task, we can define the RSF as the maximal distance Δd between the AR image and the real image with a singular fusion.

III. EXPERIMENTS

The experimental setup is set to float the virtual AR image via the beam splitter with a projection distance L = 1200 mm (0.83 diopter (D)) from the observer, which is set to be similar to the viewing condition of current combiner-type commercial HUDs. The gap Δd between the AR image and the real image varies from -0.21 D to 0.21 D

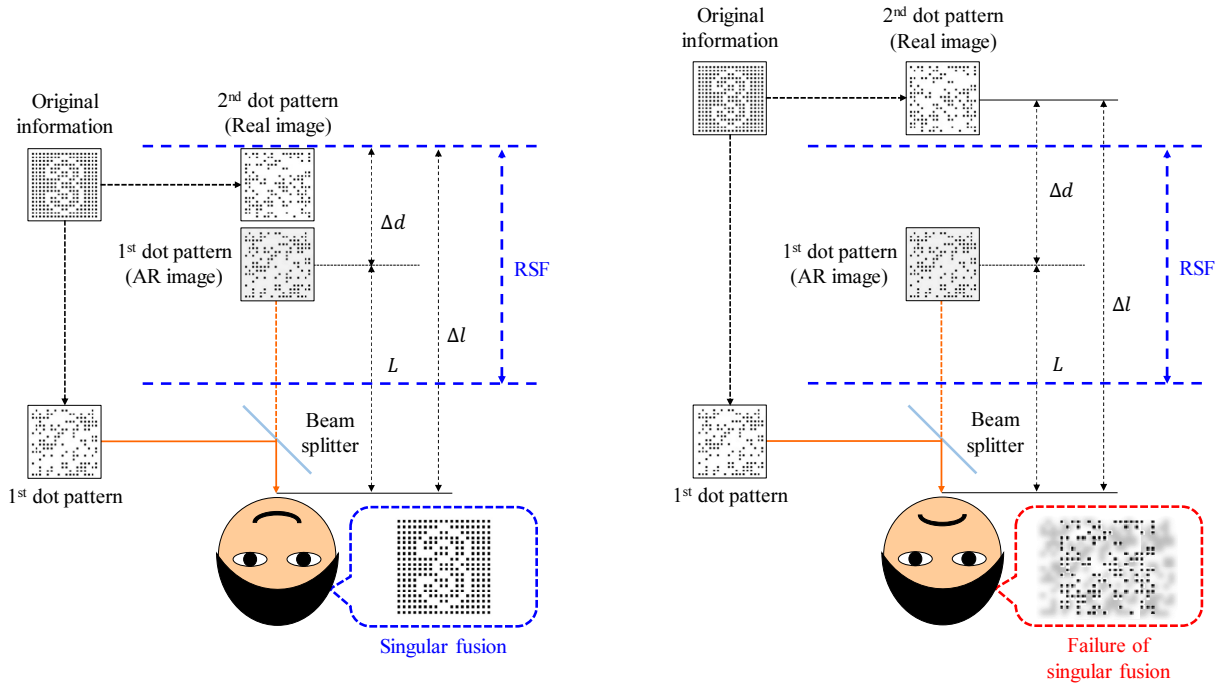

FIG. 4. Design of experimental scheme to check a success/ failure of singular fusion by a recognition of two randomly encoded dot patterns as the AR image and the real image: (a) a case with a success of singular fusion and (b) a case with a failure of singular fusion.

TABLE 1. Experimental conditions with varying Δd

Experimental conditions	L		Δd		Δl	
	D	mm	D	mm	D	mm
1	0.83	1200	-0.21	404	0.62	1604
2			-0.18	331	0.65	1531
3			-0.15	263	0.68	1463
4			-0.12	202	0.71	1402
5			-0.09	145	0.74	1345
6			-0.06	93	0.77	1293
7			-0.03	45	0.80	1245
8			0.00	0	0.03	1200
9			+0.03	-42	0.86	1158
10			+0.06	-81	0.89	1119
11			+0.09	-117	0.92	1083
12			+0.12	-151	0.95	1049
13			+0.15	-183	0.98	1017
14			+0.18	-213	1.01	987
15			+0.21	-242	1.04	958

(from 404 mm to -242 mm) with an interval of 0.03 D to provide 15 steps of difference as shown in Table 1. The dot patterns are composed of 18 by 18 black and white dots and have an angular size of approximately 3 degree (actual size of 60 mm when $\Delta l = 1200$ mm) to guarantee a

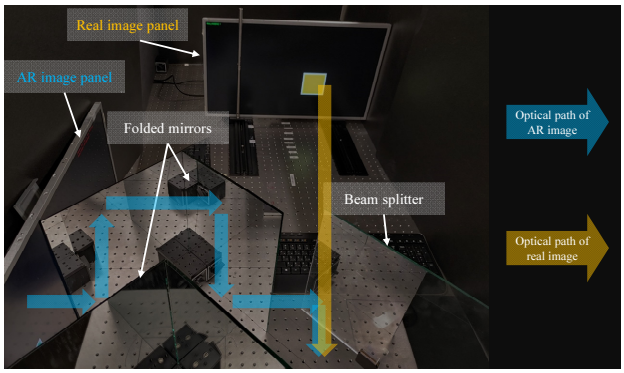

FIG. 5. Picture of experimental setup to provide the AR and the real images.

condition of central gaze. In the experiments, seven subjects between the ages of 24-28 with normal vision have participated and we collected their responses for each experimental condition (Δd) for analysis.

The picture of the experimental setup is shown in Fig. 5. The basic structure of the setup consists of two display panels, a beam splitter, and folded mirrors. The AR image and the real images are displayed on the corresponding display panels and combined by the beam splitter to be observed. The folded mirrors are used to reduce the volume of the setup as for commercial HUDs. For each experimental condition with different Δd, the angular sizes of the AR image and the real image were matched by adjusting the actual size of the real image while fixing that of the

AR image to be approximately 60 mm. For that purpose, we used two 28-inch 4K (3840 × 2160) display panels with pixel pitch of 0.162 mm since an accurate size control of the real image by an order of a single pixel pitch is necessary for a correct matching of angular sizes. The other parameters such as luminance, contrast, and color of two dot patterns (the AR image and the real image) were also matched to image to prevent unexpected distortion.

With the experimental setup described above, first we let the subjects use only a monocular vision to analyze the effect of accommodation only. The purpose of the monocular vision test is to check whether the range of experimental conditions Δd is really within the Percival's zone of comfort by analyzing the effect of accommodation only [12]. The experimental results in Fig. 6(a) show that all subjects reported a 100% correct proportion for all experimental conditions except an irregular case when Δd is +0.18 D. However, since the average proportion correct of that irregular case is also approximately 100%, we can expect that all subjects felt almost no difficulty in combining the AR image and the real image regardless of the varying gap Δd between them. Besides, the average time to respond was also recorded and plotted in Fig. 6(b). The results in Fig. 6(b) indicate that all subjects have spent about one second before responding for all Δd. Thus, from the results in Figs. 6(a) and 6(b) showing cases of the monocular vision test, we can confirm that both the AR and the real images were well combined by the observer for all conditions of Δd from -0.21 D to +0.21 D in our experimental scheme. In other words, we can experimentally confirm through the monocular vision test that the varying range of experimental conditions Δd is within the Percival's zone of comfort and the A-V mismatch will not be a major concern in the next tests using binocular vision. Therefore, we can focus on

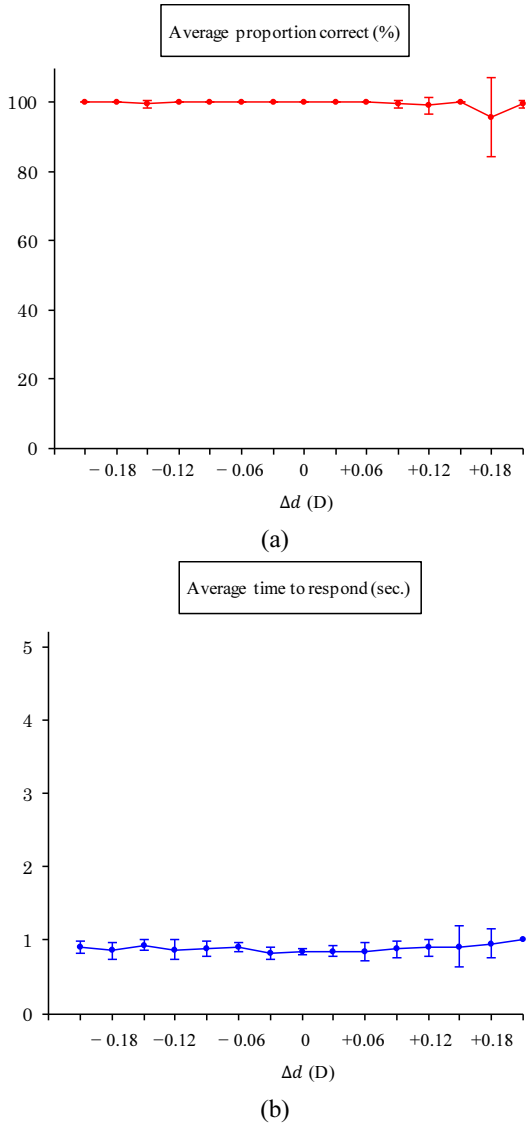

FIG. 6. The experimental results based on monocular vision: (a) average proportion correct and (b) average time to respond.

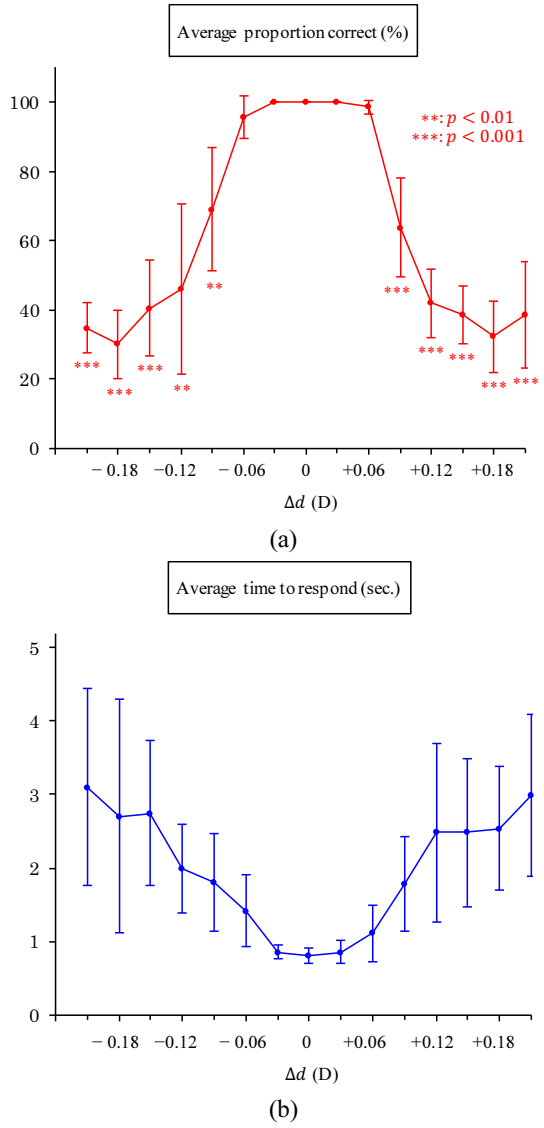

FIG. 7. The experimental results based on binocular vision: (a) average proportion correct and (b) average time to respond.

binocular fusion for the next tests.

The experimental results of binocular vision tests are shown in Fig. 7(a). As denoted above, the binocular fusion is a major factor to affect the result. Thus, it is expected that the results in Fig. 7(a) have a correlation with the RSF to induce a singular fusion. In Fig. 7(a), unlike the case in Fig. 6(a), the results show a clear tendency that the average proportion correct decreases steeply when $|\Delta d|$ is over 0.06 D. The statistical analysis based on p-value also shows that the subjects were able to report a correct answer within that range only when Δd is from -0.06 D to +0.06 D. Therefore, based on these results, we can assume that the RSF with the given experimental scheme is within the range of $|\Delta d| < 0.06$ D. In addition, it should be also notified that the derived RSF is narrower than the previous studies about the zone of comfort, which means that the A-V mismatch is not the only concern to induce visual discomfort [12, 13]. Besides, the average times to respond are shown in Fig. 7(b) with a tendency which is clearly different with the results in Fig 6(b). Though the large variances of the results in Fig. 7(b) make the statistical analysis impossible, we can still expect that they reflect the difficulty in decoding the original information due to the failure of singular fusion. Though the RSF can be changed when the blurring and misalignment will be less severe as the projection distance L is increased, we expect that the RSF is still meaningful for that case since there will be a certain misalignment between the AR images and the ambient objects.

IV. CONCLUSION

A singular fusion of the AR image and the ambient object is essential to reduce the visual fatigue of the observer using AR applications. However, current 2D AR devices cannot satisfy that condition due to the fixed position of the focal plane where the 2D planar AR image is projected. Thus, various approaches of 3D AR devices were announced to resolve the problem above by controlling the depths of AR images to match the locations of them with the ambient objects. In this paper, we designed a task-based experimental scheme and derived the RSF within which the AR image and the real object can be combined together through a singular fusion without a visual discomfort. Though there have been previous studies about the comfort zone of binocular visual stimuli [1, 12], our study has a novel impact covering a viewing condition of current commercial AR application such as HUD, which had not been considered in previous studies. Though a case with fixed projection distance was analyzed in this paper, more analysis with various positions of the AR image and the ambient object will be meaningful as future studies. We expect that the results can be helpful for the development of advanced 3D AR devices with low visual discomfort.

ACKNOWLEDGMENT

This work was supported in part by the Information Technology Research Center (ITRC) support Program supervised by the Institute for Information and Communications Technology Promotion (IITP) under Grant IITP-2017-2015-0-00448, and in part by the Basic Science Research Program through the National Research Foundation of Korea (NRF) funded by the Ministry of Education under Grant 2018R1D1A1B07049563. We also thank Dr. Joohwan Kim and Dr. Jae-Hyun Jung for their valuable comments and advice.

REFERENCES

1. K. N. Ogle, *Researches in Binocular Vision* (W. B. Saunders, Philadelphia, USA, 1950).
2. C. Jang, K. Bang, S. Moon, J. Kim, S. Lee, and B. Lee, "Retinal 3D: augmented reality near-eye display via pupil-tracked light field projection on retina," ACM Trans. Graph. **36**, 190 (2017).
3. J. Hong, S.-W. Min, and B. Lee, "Integral floating display systems for augmented reality," Appl. Opt. **51**, 4201-4209 (2012).
4. H. Hua and B. Javidi, "A 3D integral imaging optical see-through head-mounted display," Opt. Express **22**, 13484-13491 (2014).
5. Y. Takaki and Y. Yamaguchi, "Flat-panel type see-through three-dimensional display based on integral imaging," Opt. Lett. **40**, 1873-1876 (2015).
6. Y. Yamaguchi and Y. Takaki, "See-through integral imaging display with background occlusion capability," Appl. Opt. **55**, A144-A149 (2016).
7. H.-J. Yeom, H.-J. Kim, S.-B. Kim, H. Zhang, B. Li, Y.-M. Ji, S.-H Kim, and J.-H Park, "3D holographic head mounted display using holographic optical elements with astigmatism aberration compensation," Opt. Express **23**, 32025-32034 (2015).
8. G. Li, D. Lee, Y. Jeong, J. Cho, and B. Lee, "Holographic display for see-through augmented reality using mirror-lens holographic optical element," Opt. Lett. **41**, 2486-2489 (2016).
9. K. Hong, J. Yeom, C. Jang, J. Hong, and B. Lee, "Full-color lens-array holographic optical element for three-dimensional optical see-through augmented reality," Opt. Lett. **39**, 127-130 (2014).
10. K. Hong, J. Yeom, C. Jang, G. Li, J. Hong, and B. Lee, "Two-dimensional and three-dimensional transparent screens based on lens-array holographic optical elements," Opt. Express **22**, 14363-14374 (2014).
11. G. Kramida, "Resolving the vergence-accommodation conflict in head-mounted displays," IEEE Trans. Vis. Comput. Graph. **22**, 1912-1931 (2016).
12. A. S. Percival, "The relation of convergence to accommodation and its practical bearing," Ophthal. Rev. **11**, 313-328 (1892).
13. T. Shibata, J. Kim, D. M. Hoffman, and M. S. Banks, "The zone of comfort: Predicting visual discomfort with stereo displays," J. Vis. **11**, 11 (2011).